J|A|C|S ARTICLES

Published on Web 07/17/2009

Mixed Valence Europium Nitridosilicate Eu_2SiN_3

Martin Zeuner,[†] Sandro Pagano,[†] Philipp Matthes,[†] Daniel Bichler,[†] Dirk Johrendt,[†] Thomas Harmening,[‡] Rainer Pöttgen,[‡] and Wolfgang Schnick*[,†]

Ludwig-Maximilians-Universität München, Department Chemie und Biochemie, Butenandtstraße 5-13 (D), D-81377 München, Germany, and WWU Münster, Institut für Anorganische und Analytische Chemie and NRW Graduate School of Chemistry der Westfälischen Wilhelms-Universität, Germany

Received May 25, 2009; E-mail: wolfgang.schnick@uni-muenchen.de

Abstract: The mixed valence europium nitridosilicate Eu_2SiN_3 has been synthesized at 900 °C in welded tantalum ampules starting from europium and silicon diimide $Si(NH)_2$ in a lithium flux. The structure of the black material has been determined by single-crystal X-ray diffraction analysis (*Cmca* (no. 64), $a = 542.3(11)$ pm, $b = 1061.0(2)$ pm, $c = 1162.9(2)$ pm, $Z = 8$, 767 independent reflections, 37 parameters, $R1 = 0.017$, $wR2 = 0.032$). Eu_2SiN_3 is a chain-type silicate comprising one-dimensional infinite nonbranched *zweier* chains of corner-sharing SiN_4 tetrahedra running parallel [100] with a maximum stretching factor $f_s = 1.0$. The compound is isostructural with Ca_2PN_3 and Rb_2TiO_3, and it represents the first example of a nonbranched chain silicate in the class of nitridosilicates. There are two crystallographically distinct europium sites (at two different Wyckoff positions 8*f*) being occupied with Eu^{2+} and Eu^{3+}, respectively. ^{151}Eu Mössbauer spectroscopy of Eu_2SiN_3 differentiates unequivocally these two europium atoms and confirms their equiatomic multiplicity, showing static mixed valence with a constant ratio of the Eu^{2+} and Eu^{3+} signals over the whole temperature range. The Eu^{2+} site shows magnetic hyperfine field splitting at 4.2 K. Magnetic susceptibility measurements exhibit Curie−Weiss behavior above 24 K with an effective magnetic moment of 7.5 μ_B/f.u. and a small contribution of Eu^{3+}, in accordance with Eu^{2+} and Eu^{3+} in equiatomic ratio. Ferromagnetic ordering at unusually high temperature is detected at $T_C = 24$ K. DFT calculations of Eu_2SiN_3 reveal a band gap of ∼0.2 eV, which is in agreement with the black color of the compound. Both DFT calculations and lattice energetic calculations (MAPLE) corroborate the assignment of two crystallographically independent Eu sites to Eu^{2+} and Eu^{3+}.

Introduction

During the last decade nitridosilicates and oxonitridosilicates emerged from structural ceramics to advanced optical materials. Due to their exceptional chemical and physical stability in conjunction with nonlinear optical properties (e.g., 2-photon excitation, second harmonic generation, SHG) or luminescence (upon doping with Ce^{3+} or Eu^{2+}) these materials found industrial application, e.g. as highly efficient phosphors in modern LED technology.[1−7]

From a structural point of view, nitridosilicates represent a significant extension of the broad and varied crystal chemistry of classical oxosilicates, although on a local atomic scale, both oxosilicates and nitridosilicates are made up of analogous and isosteric building blocks, namely SiO_4 and SiN_4 tetrahedra, respectively. The broad diversity of condensed silicate structures is a direct consequence of the variability in connectivity of oxygen in classical silicates and even more of nitrogen in nitridosilicates.[2] Whereas the structural chemistry of oxosilicates is limited to terminal $O^{[1]}$ atoms and simply bridging $O^{[2]}$, nitridosilicates emulate the same with $N^{[1]}$ atoms and $N^{[2]}$ but can additionally form highly crosslinked networks which contain $N^{[3]}$ or $N^{[4]}$ bridges connecting three or even four neighboring tetrahedral centers (e.g., $BaYbSi_4N_7$).[8,9] Additionally, in nitridosilicates, edge sharing has been observed (e.g., $Ba_5Si_2N_6$; $BaSi_7N_{10}$).[10,11] The crystal chemistry of silicates has become much richer by introducing nitrogen atoms as anionic network formers, yielding new structure types that are naturally not occurring in minerals. Examples for such nitrido- or oxonitridosilicates are the framework silicates $M_2Si_5N_8$ (M = Ca, Sr, Ba) or also the layer silicates $MSi_2N_2O_2$ (M = Ca, Sr, Ba, Eu).[12−16] Both series of compounds proved to be excellent host

[†] Ludwig-Maximilians-Universität München.
[‡] Westfälische Wilhelms-Universität (WWU Münster).

(1) Schnick, W. *Int. J. Inorg. Mater.* **2001**, *3*, 1267.
(2) Schnick, W.; Huppertz, H. *Chem.—Eur. J.* **1997**, *3*, 679.
(3) Li, Y. Q.; deWith, G.; Hintzen, H. T. *J. Solid State Chem.* **2008**, *181*, 515.
(4) Mueller-Mach, R.; Mueller, G.; Krames, M. R.; Höppe, H. A.; Stadler, F.; Schnick, W.; Juestel, T.; Schmidt, P. *Phys. Status Solidi A* **2005**, *202*, 1727.
(5) Piao, X.; Horikawa, T.; Hanzawa, H.; Machida, K. *Appl. Phys. Lett.* **2006**, *88*, 161908.
(6) Xie, R.-J.; Hirosaki, N. *Sci. Technol. Adv. Mater.* **2007**, *8*, 588.
(7) Xie, R.-J.; Hirosaki, N.; Kimura, N.; Sakuma, K.; Mitomo, M. *Appl. Phys. Lett.* **2007**, *90*, 191101/1.
(8) Huppertz, H.; Schnick, W. *Angew. Chem.* **1996**, *108*, 2115. Huppertz, H.; Schnick, W. *Angew. Chem. Int. Ed. Engl.* **1996**, *35*, 1983.
(9) Huppertz, H.; Schnick, W. *Z. Anorg. Allg. Chem.* **1997**, *623*, 212.
(10) Yamane, H.; DiSalvo, F. J. *J. Alloys Compd.* **1996**, *240*, 33.
(11) Huppertz, H.; Schnick, W. *Chem.—Eur. J.* **1997**, *3*, 249.
(12) Höppe, H. A.; Stadler, F.; Oeckler, O.; Schnick, W. *Angew. Chem.* **2004**, *116*, 5656. Höppe, H. A.; Stadler, F.; Oeckler, O.; Schnick, W. *Angew. Chem. Int. Ed.* **2004**, *43*, 5540.

10.1021/ja9040237 CCC: $40.75

structures for rare earth doping and provide highly efficient luminescent materials which are industrially applied in commercial phosphor-converted pc-LEDs.[4,17] Even reduced nitridosilicates MSi_6N_8 with M = Sr,[18] Ba[19] exhibiting a Si−Si bond have been observed. On the majority highly condensed (oxo)nitridosilicates are obtained, due to the high possible degree of crosslinking, leading predominantly to three-dimensional networks. The synthesis and characterization of nitridosilicates with a low degree of condensation is challenging due to their high sensitivity to oxygen or moisture. The oxonitridosilicate $Gd_3[SiN_3O]O$[20] represents a nitridic example of an orthosilicate, while $Ba_5Si_2N_6$[10] exhibits a group silicate structure composed of pairs of edge-sharing tetrahedra (cf. $Ca_5[Si_2N_6]$ and $Ca_7[NbSi_2N_9]$).[21] *Schleid et al.* reported $Pr_9Se_6[Si_3N_9]$, the only known nitrido-cyclo-trisilicate so far.[22] Very recently, $M_5Si_3N_9$ (M = La, Ce) the first nitridosilicate with a chain-like Si−N substructure was reported.[23] The compound is built up of alternating Q^2- and Q^3-type corner-sharing $[SiN_4]$ tetrahedra with additional corner-sharing Q^1-units attached to the Q^3-tetrahedra, forming branched, zipper-like chains.

The combination of nitridosilicate anionic host structures with mixed valence Eu cations is an unknown phenomenon. In the year 1997 *Huppertz et al.* reported on the first nitridosilicate ($EuYbSi_4N_7$), comprising Eu^{2+} and Yb^{3+} cations.[24] More recently, *Hintzen et al.* mentioned the isostructural compound $EuYSi_4N_7$.[25] SIALON substitution variants $EuLn[Si_{4-x}Al_xO_xN_{7-x}]$ with Ln^{3+} = Ho−Yb have been extensively investigated by *Lieb et al.*[26] A different nitridosilicate $BaEu(Ba_{0.5}Eu_{0.5})YbSi_6N_{11}$ was reported by *Huppertz*,[27] containing alkaline earth and rare earth ions in a three-dimensional network structure of vertex-sharing $[SiN_4]$ tetrahedra.

In this contribution we describe the synthesis, crystal structure, and magnetic properties of the mixed valence chain-type nitridosilicate Eu_2SiN_3 comprising both Eu^{2+} as well as Eu^{3+}.

Experimental Section

Unless otherwise stated, all manipulations were performed with rigorous exclusion of oxygen and moisture in flame-dried Schlenk-type glassware on a Schlenk line, interfaced to a vacuum line (10^{-3} mbar), or in an argon-filled glove box. Argon (Messer-Griessheim, 5.0) was purified by passage over columns of silica gel (Merck), molecular sieve (Fluka, 4 Å), KOH (Merck, ≥ 85 %), P_4O_{10} (Roth, ≥99 %, granulate) and a titanium sponge at 700 °C (Johnson Matthey, 99.5 %, grain size ≤ 0.8 cm).

Table 1. Crystal Data of Eu_2SiN_3

formula	Eu_2SiN_3
formula weights [g·mol^{-1}]	374.04
crystal system	orthorhombic
space group	*Cmca* (No. 64)
diffractometer type	Nonius Kappa-CCD
radiation λ [pm]	70.930 (Mo−K_α)
crystal size [mm^3]	0.05 mm × 0.05 mm × 0.04 mm
unit cell dimensions	
a [pm]	542.3(11)
b [pm]	1061.0(2)
c [pm]	1162.9(2)
cell volume [10^6 pm^3]	669.1(2)
formula units *Z*	8
ρ [g·cm^{-3}]	7.43
F(000)	1288
μ [mm^{-1}]	37.3
temperature [K]	200(2)
θ range [deg]	3.1−34.4
absorption correction	multi-scan (SADABS)[30]
measured reflections	7709
independent reflections	768
observed reflections	749 ($F_o^2 \geq 2\sigma(F_o^2)$)
no. of refined parameter	37
min/max $\Delta\rho_e$ [e Å^{-3}]	−1.22/1.35
goodness of fit	1.182
R_1/R_1 (all data)	0.0159/0.0167
wR2 (all data)	0.0320
weighting details	$w^{-1} = \sigma^2F_o^2 + (0.0P)^2 + 4.760P$ $P = (F_o^2 + 2F_c^2)/3$

Eu_2SiN_3 was synthesized from 130.6 mg (0.86 mmol) europium (Smart-Elements, 99.9 %, pieces), 25 mg (0.43 mmol) silicon diimide (synthesized according to the reference 28), 19.8 mg Li (2.86 mmol) and 14.0 mg LiN_3 (0.29 mmol) in tantalum crucibles (wall thickness 0.5 mm, internal diameter 10 mm, length 300 mm). The latter were arc-welded under a pressure of 1 bar purified argon. The crucible holder was water-cooled in order to avoid a start of the reaction during welding. The crucible was placed in a silica tube (under argon) inside the middle of a tube furnace. The temperature was raised to 900 °C (rate 120 °C·h^{-1}), maintained for 24 h, subsequently cooled to 500 °C (rate 5 °C·h^{-1}), and finally quenched to room temperature by switching off the furnace. Eu_2SiN_3 crystallizes in black crystals, which hydrolyze rapidly after exposure to air or moisture.

Single-crystal X-ray data were collected on a Nonius Kappa-CCD diffractometer with graphite-monochromated Mo−K_α radiation (λ = 70.93 pm) with graded multilayer X-ray optics. The structure was solved by direct methods using SHELXS-97[29] and refined with anisotropic displacement parameters by full-matrix least-squares calculations on F^2 (SHELXL-97)[29] in the orthorhombic space group *Cmca* (no. 64). Details of the X-ray data collection, structural refinements, final atomic coordinates and equivalent displacement parameters are listed in Tables 1, 2, and 3 (the CIF file can be found in the Supporting Information). The data were semi-empirically corrected for absorption by using the software SADABS.[30] Further details of the crystal structure investigations can be obtained from the Fachinformationszentrum Karlsruhe, 76344 Eggenstein-Leopoldshafen, Germany (fax: (+49)7247-808-666; E-mail: crysdata@fiz-karlsruhe.de) on quoting the depository number CSD-420679.

(13) Oeckler, O.; Stadler, F.; Rosenthal, T.; Schnick, W. *Solid State Sci.* **2007**, *9*, 205.
(14) Schlieper, T.; Milius, W.; Schnick, W. *Z. Anorg. Allg. Chem.* **1995**, *621*, 1380.
(15) Schlieper, T.; Milius, W.; Schnick, W. *Z. Anorg. Allg. Chem.* **1995**, *621*, 1037.
(16) Stadler, F.; Oeckler, O.; Höppe, H. A.; Möller, M. H.; Pöttgen, R.; Mosel, B. D.; Schmidt, P.; Duppel, V.; Simon, A.; Schnick, W. *Chem.−Eur. J.* **2006**, *12*, 6984.
(17) Bachmann, V.; Ronda, C.; Oeckler, O.; Schnick, W.; Meijerink, A. *Chem. Mater.* **2009**, *21*, 316.
(18) Stadler, F.; Oeckler, O.; Senker, J.; Höppe, H. A.; Kroll, P.; Schnick, W. *Angew. Chem.* **2005**, *117*, 573. Stadler, F.; Oeckler, O.; Senker, J.; Höppe, H. A.; Kroll, P.; Schnick, W. *Angew. Chem. Int. Ed.* **2005**, *44*, 567.
(19) Stadler, F.; Schnick, W. *Z. Anorg. Allg. Chem.* **2007**, *633*, 589.
(20) Höppe, H. A.; Kotzyba, G.; Pöttgen, R.; Schnick, W. *J. Solid State Chem.* **2002**, *167*, 393.
(21) Ottinger, F.; Nesper, R. *Z. Anorg. Allg. Chem.* **2005**, *631*, 1597.
(22) Lissner, F.; Schleid, T. *Z. Anorg. Allg. Chem.* **2004**, *630*, 2226.
(23) Schmolke, C.; Bichler, D.; Johrendt, D.; Schnick, W. *Solid State Sci.* **2009**, *11*, 389.
(24) Huppertz, H.; Schnick, W. *Acta Crystallogr., Sect. C: Cryst. Struct. Commun.* **1997**, *53*, 1751.
(25) Li, Y. Q.; Fang, C. M.; deWith, G.; Hintzen, H. T. *J. Solid State Chem.* **2004**, *177*, 4687.
(26) Lieb, A.; Kechele, J. A.; Kraut, R.; Schnick, W. *Z. Anorg. Allg. Chem.* **2006**, *633*, 166.
(27) Huppertz, H.; Schnick, W. *Z. Anorg. Allg. Chem.* **2008**, *624*, 371.
(28) Lange, H.; Wötting, G.; Winter, G. *Angew. Chem.* **1991**, *103*, 1606. Lange, H.; Wötting, G.; Winter, G. *Angew. Chem. Int. Ed. Engl.* **1991**, *30*, 1579.
(29) Sheldrick, G. M. *Acta Crystallogr., Sect. A* **2008**, *64*, 112.
(30) Sheldrick, G. M. *SADABS, Multi-Scan Absorption Correction*, Version 2; University of Göttingen: Göttingen, Germany, 2001.

Table 2. Atomic Coordinates of Eu_2SiN_3

atom	Wyckoff	*x*	*y*	*z*	U_{eq}
Eu1	8*f*	1/2	0.04545(2)	0.35413(2)	0.00410(7)
Eu2	8*f*	0	0.14392(2)	0.57650(2)	0.00365(6)
Si1	8*f*	0	0.23623(13)	0.33629(9)	0.00099(18)
N1	8*f*	0	0.0750(4)	0.3738(3)	0.0047(6)
N2	8*e*	1/4	0.2757(4)	0.2500(4)	0.0053(4)
N3	8*f*	0	0.3326(4)	0.4564(3)	0.0055(6)

The crystal structure was verified by X-ray powder diffraction using Debye−Scherrer geometry on a STOE Stadi P powder diffractometer with Ge(111)-monochromatized Mo−$K_{\alpha1}$ radiation ($\lambda = 71.04$ pm) and double checking with patterns calculated from single crystal data (Figure S1, Supporting Information).

Scanning electron microscopy was performed on a JEOL JSM-6500F equipped with a field emission gun at an acceleration voltage of 10 kV. Samples were prepared by placing single crystals on adhesive conductive pads and subsequently coating them with a thin conductive carbon film. Each EDX spectrum (Oxford Instruments) was recorded with the analyzed area limited on one single crystal to avoid the influence of possible contaminating phases. Analysis of three spots per crystallite showed average atomic Eu/Si/O/N compositions (%) of 73.8(6):7.4(2):0:18.8(2). Despite the large standard deviations of the measurements, these results confirm the presence of the elements and are in agreement with the compositions obtained from single crystal X-ray studies (the calculated values Eu/Si/O/N are 81.3:7.5:0:12.2.

Magnetic moments were measured using a SQUID magnetometer (MPMS-XL5, Quantum Design Inc.) between 1.8 and 300 K with magnetic flux densities up to 5 tesla. A sample of about 16 mg was loaded in a gelatin capsule and fixed in a straw as sample holder. Corrections for the sample holder and the core diamagnetism[31] were applied to the data. Effective magnetic moments were calculated by fitting the corrected molar magnetic susceptibility data χ_m with the equation $\chi_m = C/(T - \theta_{CW})$ where C is the Curie-constant and θ_{CW} is the paramagnetic Curie−Weiss temperature (Weiss constant). The small magnetic contribution of the trivalent europium ions was taken into account by the Van Vleck equation using a spin−orbit coupling parameter $\zeta_{4f}(Eu^{3+})$ of 1326 cm^{-1}.[31]

The 21.53 keV transition of ^{151}Eu with an activity of 130 MBq (2% of the total activity of a ^{151}Sm:EuF_3 source) was used for the ^{151}Eu Mössbauer spectroscopy. The measurements were performed in the usual transmission geometry in commercial helium bath and flow cryostats. The temperature of the absorber could be varied from 4.2 to 300 K. The source was kept at room temperature in all experiments. The material for the Mössbauer spectroscopy investigation was the same as for the susceptibility measurements. The sample was diluted with silica and placed within a thin-walled glass container at a thickness corresponding to approximately 10 mg Eu/cm^2.

The electronic structure of Eu_2SiN_3 was studied with *ab initio* density functional theory methods[32] using the generalized gradient approximation (GGA) with the *Perdew et al.* Scheme[33] for the exchange-correlation functional. We used the WIEN2k package, which is based on a full-potential augmented-plane-wave method.[34] To correct for neglected correlation effects, we used the GGA+EECE (exact exchange of correlated electrons) method as implemented in the WIEN2k package.[35] The plane wave cutoff was set to $R_{min}{}^{MT}K_{max} = 7$, leading to 8662 plane waves. All calculations were done with 100k points in the Brillouin zone.

Results and Discussion

Crystal Structure. Eu_2SiN_3 is a chain-type nitridosilicate comprising one-dimensional infinite nonbranched *zweier* chains[36] of corner-sharing SiN_4 tetrahedra running parallel [100]. The chains of Eu_2SiN_3 exhibit a maximum stretching factor $f_s = 1$, comparable to $Zn(PO_3)_2$ ($f_s = 1.0$), Ca_2PN_3 ($f_s = 1.0$)[37,38] or Johannsenite $CaMg[Si_2O_6]$ ($f_s = 0.98$).[39] Eu_2SiN_3 is isostructural with the nitridophosphate Ca_2PN_3,[37,38] with Rb_2TiO_3[40] and the alkali oxocobaltates(IV) M_2CoO_3 with M = K, Rb, Cs.[41] It represents the first example of a nonbranched chain-type silicate in the class of nitridosilicates (Figure 1).

Details of the X-ray data collection, structural refinements, final atomic coordinates, and equivalent displacement parameters are listed in Tables 1, 2, and 3.

The Si−N bond lengths within the chains (173−177 pm) vary only in a small range, and the bridging angle Si−N−Si between the $[SiN_4]$ tetrahedra amounts to 152.11° (Figure 2).

There are two crystallographically distinct europium sites. The Eu atoms are coordinated in a distorted pentagonal bipyramidal manner by the nitrogen atoms of the $[Si_2N_6]^{10-}$ chains, whereby each Eu atom is coordinated to three chains. Charge neutrality in Eu_2SiN_3 is achieved by two valence states of the europium sites, namely Eu^{2+} and Eu^{3+} ions occupying the two different Wyckoff sites (8*f*). The Eu1 cation is coordinated by nitrogen atoms with distances ranging between 255 and 305 pm, while Eu2 exhibits N neighbors between 240 and 275 pm (Figure 3, Table 4). These differences in bond length of the two metal sites can analogously be found in the isostructural compound Ca_2PN_3 (Ca1−N: 244−300 pm; Ca2−N: 242−262 pm),[38] probably favoring the crystallization of the mixed valence compound Eu_2SiN_3 in this structure type.

These structural data already indicate that there is an ordered distribution of larger Eu^{2+} (Eu1) and smaller Eu^{3+} (Eu2). Typical distances for Eu^{2+}−N in nitridosilicates range between 260−325 pm ($Eu_2Si_5N_8$) and 293−306 pm ($EuYbSi_4N_7$).[24] These distances resemble those of the Eu1−N coordination. Since no mixed valence europium nitridosilicate besides Eu_2SiN_3 is known so far, only analogous compounds can be used for comparison. The distances for Eu^{3+}−N in EuN are 250.7 pm,[42] comparable and within the range of the values of Eu2. A rather suitable compound for comparison seems to be Eu_3O_4,[43] containing mixed valence europium which connects oxygen atoms. The distances Eu^{2+}−O (264−296 pm) are significantly longer than those of Eu^{3+}−O (230−249 pm). Compared to the Eu−N bonds in Eu_2SiN_3 the Eu−O bonds are generally shorter, due to the smaller and more electronegative oxygen. The shortest inter-

(31) Lueken, H., *Magnetochemistry*; Teubner: Stuttgart, 1999.
(32) Gonze, X.; et al. *Comput. Mater. Sci.* **2002**, *25*, 478.
(33) Perdew, J. P.; Burke, K.; Ernzerhof, M. *Phys. Rev. Lett.* **1996**, *77*, 3865.
(34) Blaha, P.; Schwarz, K.; Madsen, G. K. H.; Kvasnicka, D.; Luitz, J. *WIEN2k*, An Augmented Plane Wave + Local Orbitals Program for Calculating Crystal Properties; Technische Universität Wien: Austria, 2001.
(35) Novak, P.; Kunes, J.; Chaput, L.; Pickett, W. E. *Phys. Status Solidi B* **2006**, *243*, 563.
(36) Liebau established the terms *zweier, dreier, vierer*, *fünfer* chains. Thereby, a *zweier* chain can be described as *two* polyhedra within one repeating unit of the linear part of the chain. The terms derive from the German numbers *drei*, *vier*, *fünf* by suffixing "er" to the numeral. Liebau, F. *Structural Chemistry of Silicates*; Springer: Berlin, 1985.
(37) Schnick, W.; Schultz-Coulon, V. *Angew. Chem.* **1993**, *105*, 846. Schnick, W.; Schultz-Coulon, V. *Angew. Chem. Int. Ed. Engl.* **1993**, *32*, 806.
(38) Schultz-Coulon, V.; Schnick, W. *Z. Anorg. Allg. Chem.* **1997**, *623*, 69.
(39) Liebau, F. *Structural Chemistry of Silicates*; Springer: Berlin, 1985; p 80 ff.
(40) Schartau, W.; Hoppe, R. *Z. Anorg. Allg. Chem.* **1974**, *408*, 60.
(41) Jansen, M.; Hoppe, R. *Z. Anorg. Allg. Chem.* **1974**, *408*, 75.
(42) Klemm, W.; Winkelmann, G. *Z. Anorg. Allg. Chem.* **1956**, *288*, 87.
(43) Rau, R. C. *Acta Crystallogr.* **1966**, *20*, 716.

Table 3. Anisotropic Displacement Parameters[a] of Eu_2SiN_3

atom	U_{11}	U_{22}	U_{33}	U_{23}	U_{13}	U_{12}
Eu1	0.00461(10)	0.00428(10)	0.00340(10)	0.00056(6)	0.00000	0.00000
Eu2	0.00563(10)	0.00284(10)	0.00247(10)	−0.00005(6)	0.00000	0.00000
Si1	0.0006(4)	0.0016(5)	0.0008(4)	−0.0002(3)	0.00000	0.00000
N1	0.0070(16)	0.0030(14)	0.0040(13)	−0.0013(12)	0.00000	0.00000
N2	0.0033(13)	0.0077(15)	0.0050(13)	0.000	0.0023(11)	0.00000
N3	0.0080(16)	0.0050(15)	0.0034(14)	0.0013(12)	0.00000	0.00000

[a] The anisotropic temperature factor is given as $\exp[-2\pi^2(U_{11}h^2a^{*2} + ... + 2U_{13}hla^*c^*)]$: U_{eq} is defined as one-third of the trace of the U_{ij} tensor.

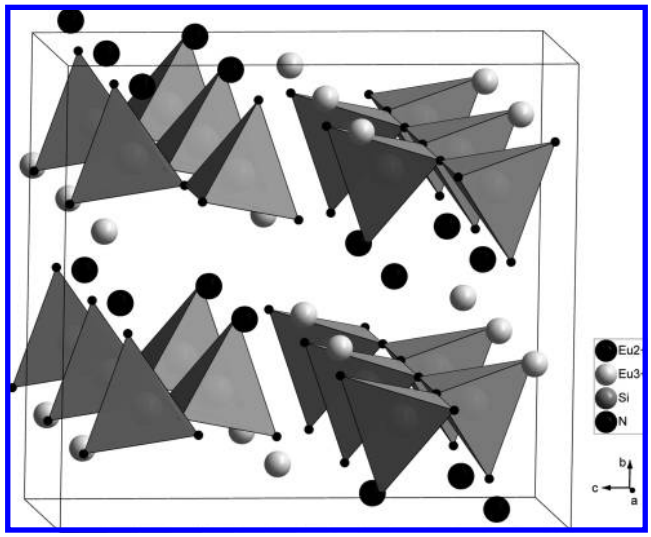

Figure 1. Perspective view of Eu_2SiN_3 along [100].

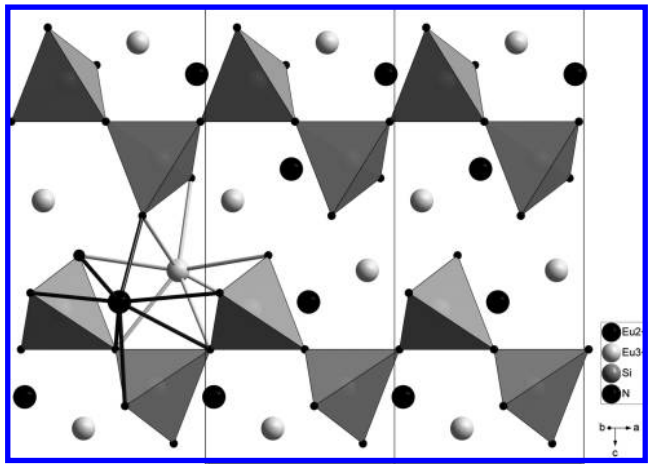

Figure 2. View along the $[Si_2N_6]_n^{10-}$ chains of Eu_2SiN_3. The two Eu sites connect three chains with one another.

atomic distance between the europium sites is 339 pm which resembles those in $Eu_2Si_5N_8$ (341.7 pm)[24] and EuN (354.8 pm).[42]

Lattice Energy Calculations According to the Maple Concept. MAPLE (Madelung Part of Lattice Energy)[44] calculations were performed on Eu_2SiN_3. This method is especially useful for the mixed valence compound since it exclusively considers the electrostatic interactions in ionic crystals, depending on the distance, charge, and coordination of the constituting atoms. The MAPLE sum values of 31146 kJ·mol^{-1} were

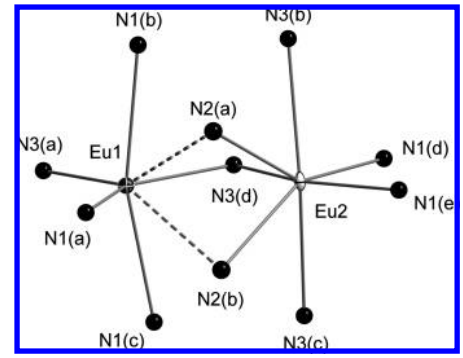

Figure 3. Nitrogen coordination of Eu1 and Eu2 in Eu_2SiN_3 (ellipsoids with a probability of 90 %).

Table 4. Selected Interatomic Distances [pm] and Angles [deg] in Eu_2SiN_3 (standard deviation in parentheses)

Eu1−Eu2	339.3(6) pm	Si−N1	173.3(3) pm
Eu1−N1(a)	267.2(1) pm	Si−N2	176.4(3) pm
Eu1−N1(b)	274.0(1) pm	Si−N3	173.8(2) pm
Eu1−N1(c)	274.0(1) pm		
Eu1−N2(a)	304.5(1) pm	Si−N2−Si	152.1(2) deg
Eu1−N2(b)	304.5(1) pm		
Eu1−N3(a)	255.2(1) pm		
Eu1−N3(d)	255.3(1) pm		
Eu2−Eu1	339.3(6) pm		
Eu2−N1(d)	246.5(1) pm		
Eu2−N1(e)	239.5(1) pm		
Eu2−N2(a)	257.6(1) pm		
Eu2−N2(b)	257.6(1) pm		
Eu2−N3(b)	275.0(1) pm		
Eu2−N3(c)	275.0(1) pm		
Eu2−N3(d)	244.2(1) pm		

calculated starting from the refined structural data with Eu^{2+} at the Eu1 site and Eu^{3+} at Eu2 (Table 5, Eu_2SiN_3 **1**).

The values are close to the sum of the total MAPLE values of the starting materials (difference 0.4 %). The calculated partial MAPLE values of the crystallographically different atoms are within their typical range. Especially the Eu^{3+} values compare well with calculated MAPLE values of EuN[42] or Eu_3O_4,[43] respectively. The *MAPLE values (MAPLE/charge) exhibit the same value for Eu1 = Eu^{2+} and Eu2 = Eu^{3+}, corroborating this assignment. If the occupancy of the europium sites is interchanged (Eu1 → Eu^{3+} and Eu2 → Eu^{2+}, Eu_2SiN_3 **2**), the MAPLE value of the compound differs 1.5 % to the sum of the total MAPLE values of the starting materials. Furthermore, the partial europium values change significantly to anomalous MAPLE values for Eu^{2+} and Eu^{3+}. Calculations with a charge of +2.5 on both europium sites (not displayed) revealed a favoritism of the Eu1 site for lower charges and a difference of 1.5 % to the sum of the total MAPLE values.

(44) Hübenthal, R. *MAPLE*, Programm zur Berechnung des Madelunganteils der Gitterenergie, Version 4; Universität Giessen: Giessen, 1993.

(45) Köllisch, K. Doctoral Thesis, 2001, University of Munich (LMU).

Table 5. Results of the MAPLE Calculations for Eu_2SiN_3 and Increment Calculations in kJ·mol^{-1}

Eu_2SiN_3 (**1**)	MAPLE	*MAPLE[a]	Eu_2SiN_3 (**2**)	MAPLE	*MAPLE[a]
Eu1 = Eu^{2+}	1910	478	Eu1 = Eu^{3+}	3754	417
Eu2 = Eu^{3+}	4254	473	Eu2 = Eu^{2+}	2228	557
Si	9960		Si	10018	
N1	4785		N1	4786	
N2	5459		N2	5396	
N3	4778		N3	4637	

Typical Partial MAPLE[45] Values[b]				
MAPLE (EuN + 1/2 $Eu_2Si_5N_8$ − 1/2 Si_3N_4)	MAPLE Eu_2SiN_3 (**1**) Eu1 = Eu^{2+}; Eu2 = Eu^{3+}		MAPLE Eu_2SiN_3 (**2**) Eu1 = Eu^{3+}; Eu2 = Eu^{2+}	
31270	31146	Δ^c = 0.4%	30819	Δ^c = 1.5%

[a] MAPLE/charge. [b] Eu^{2+}: 1900−2000; Eu^{3+}: 4000−5000; Si^{4+}: 9000−10200; N^{3-}: 5000−6000. [c] Δ = difference.

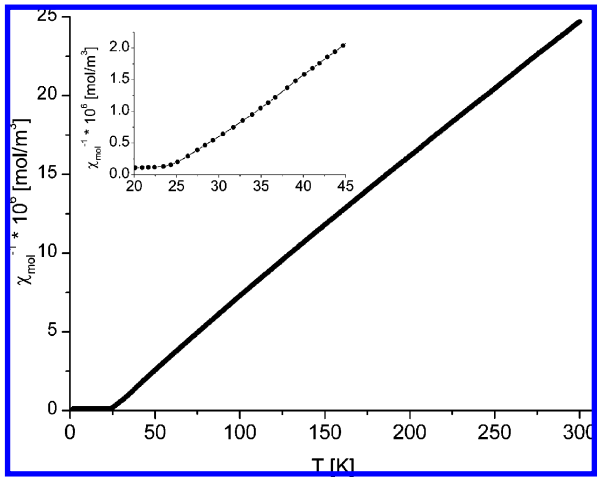

Figure 4. Temperature dependence of the inverse magnetic susceptibility of Eu_2SiN_3 measured at 0.1 T. The low-temperature behavior is shown in the inset.

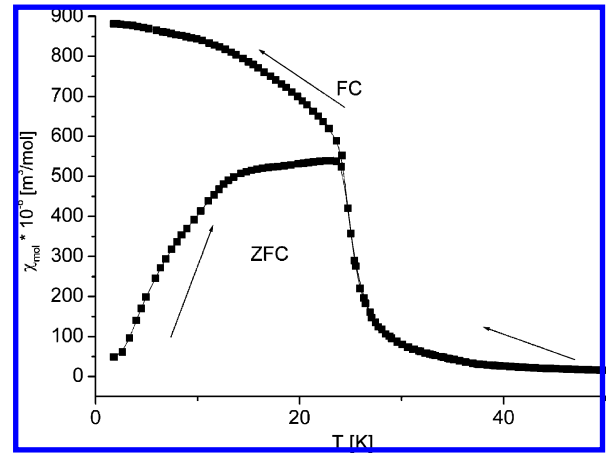

Figure 5. Low-temperature susceptibility of Eu_2SiN_3 measured at an external field strength of 0.003 T in the zero-field-cooling (ZFC) and field-cooling (FC) modus. Ferromagnetic behavior below T_C = 24 K can be observed.

Magnetic Measurements. The temperature dependence of the inverse magnetic susceptibility measured at magnetic flux density of 0.1 T is shown in Figure 4.

By fitting the $1/\chi$ (T) data using the Curie−Weiss law only, we obtain an effective magnetic moment μ_{eff} = 8.12 μ_B per formula unit, which is too high compared with 7.94 μ_B as expected for Eu^{2+}. By considering the Van Vleck contribution of the Eu^{3+} ions with a fixed spin-orbit coupling parameter ζ_{4f} of 1326 cm^{-1} taken from ref 31, the fit resulted in an effective magnetic moment of 7.5 μ_B. This is in good agreement with Eu^{2+} if we bear in mind the crystal field dependency of the ζ_{4f} parameter. We were not able to obtain a reliable fit of ζ_{4f} from our data; thus, our approach is only an estimation of the small, but noticeable, Eu^{3+} contribution. The valence combinations $Eu^{2+}Eu^{2+}SiN_3$ or $Eu^{3+}Eu^{3+}SiN_3$ would exhibit magnetic moments of 11.2 μ_B and ∼0 μ_B, respectively, underlining the presence of mixed valence europium in Eu_2SiN_3.

The positive Weiss constant (θ_{CW} = 28 K) is indicative of ferromagnetic interactions. Subsequent zero-field-cooled (ZFC) and field-cooled (FC) measurements at a magnetic flux density of 3 mT (Figure 5) confirmed the ferromagnetic behavior below T_C = 24 K.

The Curie temperature of Eu_2SiN_3 is rather high compared to other ferromagnetic Eu compounds, as collected in Table 6. Europium oxide EuO exhibits a very high T_C value compared to the higher homologue EuS. Europium silicates typically show lower values within the range of the nitridosilicate $Eu_2Si_5N_8$.[46]

Table 6. Curie Temperatures and Weiss Constants of Eu_2SiN_3 and Selected Eu Compounds

group	compound	T_C [K]	θ [K]
(oxo)nitridosilicates	Eu_2SiN_3	24	28
	$Eu_2Si_5N_8$[46]	13	18
	$EuSi_2O_2N_2$[16]	4.5	2.2
silicates	Eu_2SiO_4[47]	10	10
	Eu_3SiO_5[47]	19	19
oxides	EuO[48]	69	76
sulfides	EuS[48]	16	19
halides	EuI_2[48]	5	5

We have finally measured the isothermal magnetization at 1.8, 25, 50, and 100 K (Figure 6). The magnetizations increase linearly at 50 and 100 K, as expected for a paramagnetic compound. Close to the magnetic ordering temperature, the curve is much steeper, and the bend indicates the onset of magnetic ordering.

At 1.8 K, the magnetization is almost saturated close to 6.5 μ_B/f.u. at 5 T, in very good agreement with the theoretical value of 7 μ_B/f.u. for one Eu^{2+} and one Eu^{3+} atom according to $g_J \times J$.[31] Two Eu^{2+} sites would exhibit much higher values around

(46) Höppe, H.; Trill, H.; Mosel, B. D.; Eckert, H.; Kotzyba, G.; Pöttgen, R.; Schnick, W. *J. Phys. Chem. Solids* **2002**, *63*, 853.
(47) Shafer, M. *J. Appl. Phys.* **1965**, *36*, 1145.
(48) McGuire, T.; Shafer, M. *J. Appl. Phys.* **1964**, *35*, 984.

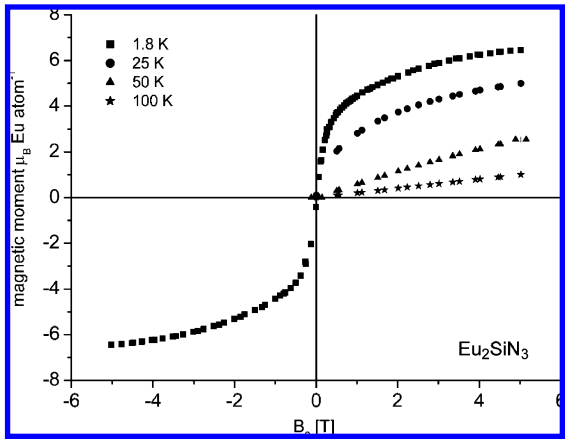

Figure 6. Magnetization versus external field strength of Eu_2SiN_3 measured at 1.8, 25, 50, and 100 K.

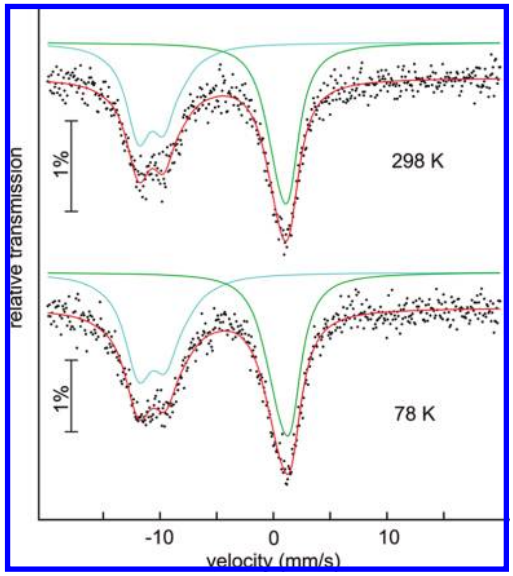

Figure 7. Experimental (red line: fitting of measured black points) and simulated (blue: Eu^{2+}; green Eu^{3+}) ^{151}Eu Mössbauer spectra of Eu_2SiN_3 at 78 and 298 K.

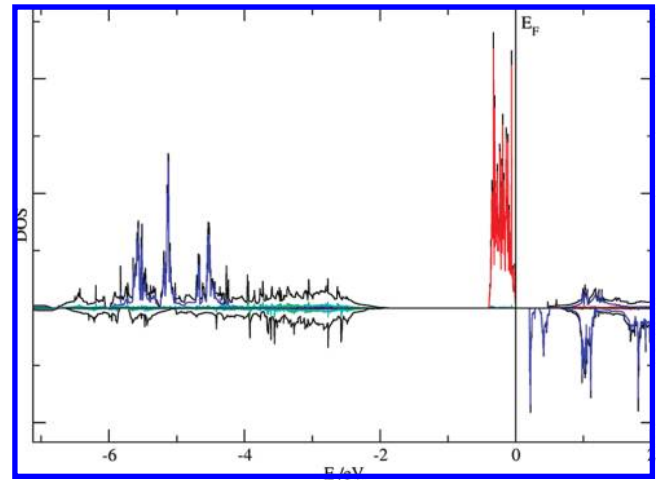

Figure 8. Density-of-states (DOS) of Eu_2SiN_3, calculated with the GGA+EECE approach. Eu1 (red); Eu2 (blue), and Si−N (turquoise) bands.

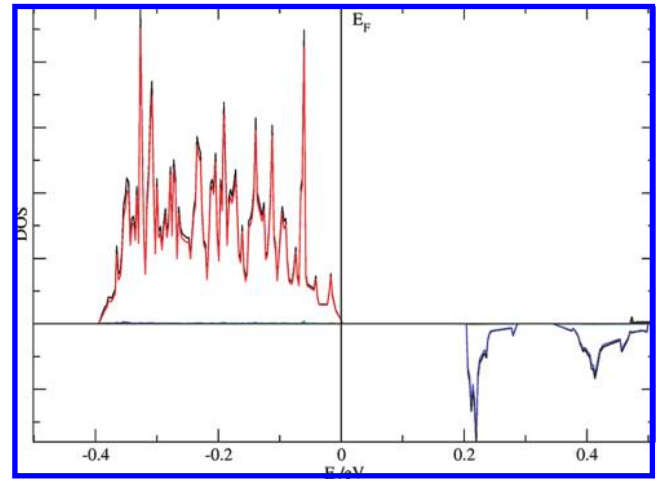

Figure 9. Density-of-states (DOS) of Eu_2SiN_3, calculated with the GGA+EECE approach. An energy gap of ∼0.2 eV discerns the differences between the bonding Eu1 (red) and antibonding Eu2 (blue) bands.

14 μ_B. The paramagnetic moment and the saturation magnetization at low temperatures are comparable to the values of the nitridosilicates $Eu_2Si_5N_8$ and $EuSi_2O_2N_2$.[16,46] With respect to the very small ferromagnetic hysteresis, Eu_2SiN_3 might be classified as a soft ferromagnet.

Mössbauer Spectroscopy. The ^{151}Eu Mössbauer spectra of Eu_2SiN_3 at 78 and 298 K are presented in Figure 7 together with transmission integral fits. The corresponding fitting parameters for these and additional measurements at other temperatures are listed in Table 7.

The spectra clearly show two well-separated signals with equal intensity. The signal at an isomer shift of −10.57 mm/s (78 K data) can be attributed to the Eu^{2+} ions. It is subject to quadrupole splitting of −7.5 mm/s, and furthermore, an asymmetry parameter of $\eta = 0.7$ was included in the fit. Compared to the recently reported nitridosilicates $Eu_2Si_5N_8$[46] (−11.88 mm/s) and $EuSi_2O_2N_2$[16] (−12.3 mm/s), Eu_2SiN_3 shows by far the smallest isomer shift. This is indicative of a higher degree of covalent bonding in Eu_2SiN_3. Gerth et al.[49] have systemized the course of the isomer shift vs. the ionicity of the respective chemical bonds. A decrease of the isomer shift (also a decrease of the electron density at the nuclei) reflects the participation of the 6s electrons in the covalent bonding. This tendency can be observed by shorter bond lengths of the Eu^{2+} site in Eu_2SiN_3 compared to $Eu_2Si_5N_8$ (260−325 pm) and $EuSi_2O_2N_2$ (280−293

Table 7. Fitting Parameters for ^{151}Eu Mössbauer Spectroscopic Measurements on Eu_2SiN_3[a]

T (K)	δ_1 (mm/s)	Γ_1 (mm/s)	ΔE_{Q1} (mm/s)	η	δ_2 (mm/s)	Γ_2 (mm/s)	ΔE_{Q2} (mm/s)	%
35	−10.67(6)	2.7(2)	−7.5(3)	0.7	0.92(5)	2.2(2)	4.2(4)	53(2)/47(2)
78	−10.57(4)	2.8(1)	−7.5(2)	0.7	0.89(3)	2.3(1)	3.9(3)	51(1)/49(1)
150	−10.76(6)	2.9(2)	−7.4(3)	0.7	0.84(4)	2.4(2)	3.0(6)	54(2)/46(2)
298	−10.66(4)	2.5(1)	−7.0(2)	0.7	0.85(4)	2.3(1)	3.2(3)	49(1)/51(1)

[a] Isomer shift (δ), electric quadrupole interaction (ΔE_Q), asymmetry parameter (η), and experimental line width (Γ). The indices 1 and 2 refer to the Eu^{2+} and Eu^{3+} sites. For details see text.

pm). The second signal at 0.89 mm/s (78 K data) is due to Eu^{3+}. The latter also shows electric quadrupole splitting, however, with a smaller absolute ΔE_Q value as compared to Eu^{2+}. Over the whole temperature range investigated (Table 7), the isomer shift values of Eu^{2+} and Eu^{3+} do not vary more than one standard deviation. This is indicative for stable static mixed valence in Eu_2SiN_3, in good agreement with the magnetic data. In contrast to $Eu_{14}Cl_{33}$[50] no temperature-dependent change in the Eu^{2+}/Eu^{3+} ratio could be observed in the Mössbauer spectra, probably due to the more rigid lattice of the nitridosilicate compound.[51] The valence behavior of Eu_2SiN_3 is similar to other static intermediate valence compounds such as Eu_2CuS_3,[52] $Eu_3F_4S_2$,[53] $Eu_5Sn_3S_{12}$,[54] or $Eu_5Zr_3S_{12}$.[55]

The Eu_2SiN_3 sample has also been measured at 4.2 K, well below the magnetic ordering temperature of $T_C = 24$ K. The divalent europium site showed magnetic hyperfine field splitting; however, although the total counting time was 5 days, the resulting spectrum had a poor signal-to-background ratio. A reliable fit of the data was not possible.

Electronic Structure Calculations. The electronic structure of Eu_2SiN_3 was studied using *ab initio* density functional theory (DFT) methods.[32] Experimental lattice parameters and atomic coordinates were used. The total density of states (DOS) together with the contributions of the Eu 5*f* orbitals as well as the silicon and nitrogen atoms is displayed in Figure 8.

The DOS just below the Fermi level is dominated by Eu1 (Eu^{2+}) 4*f* states (−0.4 to 0 eV). Above the Fermi level, we find an energy gap E_G of ∼0.2 eV between filled Eu1 and unfilled Eu2 states (Figure 9).

Since the DFT generally underestimates band gaps, the experimental gap is expected to be larger, but certainly below 1 eV due to the black color of the compound. We calculate 6.7 unpaired electrons at the Eu1 (Eu^{2+}) site and 6.0 unpaired electrons at the Eu2 (Eu^{3+}) site in very good agreement with the valence assignments suggested by the MAPLE calculations and the interatomic distances.

Conclusion

Eu_2SiN_3 features the structural motif of one-dimensional infinite nonbranched *zweier* chains, hitherto unknown in nitridosilicates, and additionally is the first representative of mixed valence nitridosilicates. Magnetic measurements revealed a magnetic moment of 7.5 μ_B/f.u. and ferromagnetic order was detected below 24 K. ^{151}Eu−Mössbauer spectroscopy confirmed the ratio Eu^{2+}/Eu^{3+} of 1:1. Lattice energy calculations (MAPLE) allowed the crude assignment of the mixed valence europium sites. A small band gap of ∼0.2 eV was determined by DFT calculations using GGA+EECE, additionally the assignment of the Eu^{2+} and Eu^{3+} sites was confirmed. Therefore, Eu_2SiN_3 may be classified as a static mixed valent europium compound, regardless of its black color, which implies some polaron activities. Further investigations about the exchange of the Eu^{3+} or Eu^{2+} ion are currently in progress, which might lead to luminescent materials with interesting magnetic properties.

Acknowledgment. We thank M. Tegel for performing the magnetic measurements, as well as Dr. Mayer for collecting the single-crystal X-ray data (both LMU Munich; Department Chemie und Biochemie). The authors gratefully acknowledge financial support by the Fonds der Chemischen Industrie (FCI) and by the Deutsche Forschungsgemeinschaft. Thomas Harmening is indebted to the NRW Graduate School of Chemistry for a research stipend.

Supporting Information Available: Complete ref 32 and XRD-pattern (Mo−$K_{\alpha1}$) of Eu_2SiN_3. This material is available free of charge via the Internet at http://pubs.acs.org.

JA9040237

(49) Gerth, G.; Kienle, P.; Luchner, K. *Phys. Lett. A* **1968**, *27*, 557.
(50) Sanchez, J. P.; Malki, M.; Friedt, J. M.; Bärnighausen, H. *Hyperfine Interact.* **1986**, *28*, 811.
(51) Bärnighausen, H. Personal message.
(52) Furuuchi, F.; Wakeshima, M.; Hinatsu, Y. *J. Solid State Chem.* **2004**, *177*, 3853.
(53) Grossholz, H.; Hartenbach, I.; Kotzyba, G.; Pöttgen, R.; Trill, H.; Mosel, B. D.; Schleid, T. *J. Solid State Chem.* **2009**, submitted.
(54) Jakubcová, P.; Johrendt, D.; Sebastian, C. P.; Rayaprol, S.; Pöttgen, R. *Z. Naturforsch.* **2007**, *62b*, 5.
(55) Jakubcová, P.; Schappacher, F. M.; Pöttgen, R.; Johrendt, D. *Z. Anorg. Allg. Chem.* **2009**, *635*, 759.